Two-Dimensional H(div)-Conforming Finite Element Spaces with hp-Adaptivity

Philippe R.B. Devloo, Agnaldo M. Farias, Sônia M. Gomes, and Denise de Siqueira

Abstract The purpose of the paper is to analyse the effect of hp mesh adaptation when discretized versions of finite element mixed formulations are applied to elliptic problems with singular solutions. Two stable configurations of approximation spaces, based on affine triangular and quadrilateral meshes, are considered for primal and dual (flux) variables. When computing sufficiently smooth solutions using regular meshes, the first configuration gives optimal convergence rates of identical approximation orders for both variables, as well as for the divergence of the flux. For the second configuration, higher convergence rates are obtained for the primal variable. Furthermore, after static condensation is applied, the condensed systems to be solved have the same dimension in both configuration cases, which is proportional to their border flux dimensions. A test problem with a steep interior layer is simulated, and the results demonstrate exponential rates of convergence. Comparison of the results obtained with H^1-conforming formulation are also presented.

1 Introduction

Several methods have been developed for the construction of $\mathbf{H}(div)$-conforming approximation spaces to be applied in flux approximations of the mixed finite element formulation. In some contexts the vector basis functions are constructed on the master element, which is mapped to the elements of the partition using Piola

P.R.B. Devloo
FEC – Universidade Estadual de Campinas, Campinas SP, Brazil
e-mail: phil@fec.unicamp.br

A.M. Farias • S.M. Gomes (✉)
IMECC – Universidade Estadual de Campinas, Campinas SP, Brazil
e-mail: agnaldofarias.mg@gmail.com; soniag@ime.unicamp.br

D.-de Siqueira
Departamento de Matemática, UTFPR 80230-901, Curitiba, PR, Brazil
e-mail: denisesiqueira@utfpr.edu.br

B. Karasözen et al. (eds.), *Numerical Mathematics and Advanced Applications ENUMATH 2015*, Lecture Notes in Computational Science and Engineering 112, DOI 10.1007/978-3-319-39929-4_9

transformations, as described in [1, 2, 8]. The constructions of hierarchical high order spaces in [5, 7, 10, 11] are based on the properties of the De Rham complex.

Another methodology is proposed in [9] for the construction of hierarchical high order $\mathbf{H}(div)$-conforming approximation spaces based on affine triangular or quadrilateral elements, which has been extended to *hp*-adaptive meshes in [6], and to three-dimensional affine tetrahedral, hexahedral and prismatic meshes in [4]. The principle is to choose appropriate constant vector fields, based on the geometry of each element, which are multiplied by an available set of H^1 hierarchical scalar basis functions to form vectorial shape functions. The assemblage of them, having the characteristic property of $\mathbf{H}(div)$-conforming functions of continuous normal components over element interfaces, is a direct consequence of the properties of the properly chosen vector fields, and of the continuity of the scalar basis functions.

As described in [4], these vectorial shape functions can be combined in different ways to form $\mathbf{H}(div)$-conforming approximation spaces to be applied for flux approximations in discretized versions of the mixed formulation for elliptic problems. In all configurations, the divergence of the dual space and the primal approximation space coincide. There is a first configuration that gives optimal convergence rates of identical approximation orders for primal and dual (flux) variables, as well as for the divergence of the flux, when computing sufficiently smooth solutions using regular meshes. For a second configuration, the accuracy of the primal variable can be enhanced by increasing its approximation order and by enriching the dual space with some properly chosen internal shape functions. Using static condensation, the global condensed matrices to be solved in these two types of space configuration have the same dimension, which is proportional to the dimension of border fluxes.

The purpose of the present paper is to analyse the effect of *hp* mesh adaptation on these space configurations when applied to singular problems. A test problem with a steep interior layer is simulated, and the results demonstrate exponential rates of convergence. Comparison of the results obtained with H^1-conforming formulation are also presented. The implementations are performed in the NeoPZ [1] computational platform, which is an open-source object-oriented project providing a comprehensive set of high performance tools for finite element simulations, including *hp* adaptivity [3].

2 Approximation Spaces in $\mathbf{H}(div, \Omega)$

Let Γ be a mesh on a domain $\Omega \subset \mathbb{R}^2$ formed by elements K. The approximation subspaces in

$$\mathbf{H}(div, \Omega) = \left\{\mathbf{q} \in L^2(\Omega) \times L^2(\Omega); \nabla.\mathbf{q} \in L^2(\Omega)\right\},$$

[1] http://github.com/labmec/neopz

which are defined piecewise over the elements of Γ, require that the local pieces $\mathbf{q}_K = \mathbf{q}|_K$ should be assembled by keeping continuous normal components across common element edges. We shall be concerned with affine triangular or quadrilateral meshes, without any limitation on hanging sides, and varying approximation order distribution $\mathbf{k} = (k_K)$. The proposed methodology used for the construction of such kind of approximation subspaces follows a sequence of steps described below. For more details, we refer to [9], in the case of regular meshes, and to [6] for the case of *hp*-adaptive meshes.

1. For each element K, there is an affine geometric mapping $\mathbf{x} : \hat{K} \to K$, associating each point $\boldsymbol{\xi} \in \hat{K}$ of the (rectangular or triangular) master element $\hat{K}$ to a point $\mathbf{p} = \mathbf{x}(\boldsymbol{\xi}) \in K$.
2. A family of hierarchical bases $\mathbf{B}^K_{k_K} = \{\boldsymbol{\Phi}\}$ is given, where the parameter k_K refers to the degree of the polynomials in $\mathscr{P}_{k_K}$ used in their definitions (of maximum degree, for quadrilateral elements, or of total degree, for triangular elements), as proposed in [9]. The principle is to choose appropriate constant vector fields $\mathbf{v}$, based on the geometry of the element, which are multiplied by an available set of H^1 hierarchical scalar basis functions φ to form a vectorial shape function $\boldsymbol{\Phi} = \varphi\hat{\mathbf{v}}$. There are shape functions of interior type, with vanishing normal components over all element edges. Otherwise, $\boldsymbol{\Phi}$ is classified as of edge type, and its normal component on the edge associated to it coincides with the restriction of the scalar shape function φ used in its definition, and vanishes over the other edges.
3. Construction of approximation subspaces of $\mathbf{H}(\mathrm{div}, \Omega)$ formed by functions $\mathbf{q} \in \left[L^2(\Omega)\right]^2$, which are defined piecewise over the elements of Γ by local functions $\mathbf{q}_K = \mathbf{q}|_K \in \mathit{span}\ \mathbf{B}^K_{k_K} \subset \mathbf{H}(\mathrm{div}, K)$. As described in [6], the pieces can be easily assembled to get continuous normal components on the elements interfaces. This property is obtained as a consequence of the particular properties satisfied by the proposed vectorial shape functions, and the continuity of the scalar shape functions used in their construction.

3 Application to Mixed Finite Element Formulation

Given $f \in L^2(\Omega)$, boundary values u_D and g for Dirichlet and Neumann conditions enforced on $\partial\Omega_D$ and $\partial\Omega_N$, consider the variational mixed formulation of finding $u \in L^2(\Omega)$ and $\boldsymbol{\sigma} \in \mathbf{V} = \{\mathbf{q} \in \mathbf{H}(div, \Omega); \boldsymbol{\sigma} \cdot \boldsymbol{\eta}|_{\partial\Omega_N} = -g\}$, such that, for all $v \in L^2(\Omega)$, and $\mathbf{q} \in \mathbf{V}_0 = \{\mathbf{q} \in \mathbf{H}(div, \Omega); \mathbf{q} \cdot \boldsymbol{\eta}|_{\partial\Omega_N} = 0\}$,

$$\int_\Omega \boldsymbol{\sigma} \cdot \mathbf{q}\, d\Omega - \int_\Omega u\, \nabla \cdot \mathbf{q}\, d\Omega = -\int_{\partial\Omega_D} u_D\, \mathbf{q} \cdot \boldsymbol{\eta}\, ds,$$

$$-\int_\Omega \nabla \cdot \boldsymbol{\sigma}\, v\, d\Omega = -\int_\Omega f v\, d\Omega.$$

Approximation Spaces Following the developments in [4], we shall consider two stable configuration cases for approximation spaces to be used for primal u and dual $\boldsymbol{\sigma}$ variables in discretized versions of the mixed formulation. In both cases, the primal variable is approximated in subspaces of $L^2(\Omega)$ formed by piecewise functions $u|_K = u_K$, without any continuity constraint, as in typical discretized mixed formulations [2].

The first configuration considers polynomials $u_K \in \mathscr{P}_{k_K}$, and the dual variable $\boldsymbol{\sigma}$ is sought in approximation spaces $\subset \mathbf{H}(div, \Omega)$ formed by vectorial functions $\mathbf{q}$ such that $\boldsymbol{q}_K = \boldsymbol{q}|_K \in span\ \mathbf{B}_{k_K}^{K*}$, where the bases $\mathbf{B}_{k_K}^{K*} \subset \mathbf{B}_{k_K+1}^{K}$ are formed by enriching $\mathbf{B}_{k_K}^{K}$ with interior shape functions $\boldsymbol{\Phi} \in \mathbf{B}_{k_K+1}^{K}$ whose divergence $\nabla \cdot \boldsymbol{\Phi} \in \mathscr{P}_{k_K}$. The resulting set of approximations spaces is classified as being of $\mathbf{P}_{\mathbf{k}}^{*}\ P_{\mathbf{k}}$ type.

Another type of approximation configuration is classified as being of $\mathbf{P}_{\mathbf{k}}^{**}\ P_{\mathbf{k}+1}$ type, where the primal approximations u_K are in $\mathscr{P}_{k_K+1}$, and $\mathbf{P}_{k}^{**}$ refers to vectorial approximation spaces spanned by bases $\mathbf{B}_{k_K}^{K**} \subset \mathbf{B}_{k_K+1}^{K*}$, where the edge functions are restricted to those ones of $\mathbf{P}_{\mathbf{k}}^{*}$ type.

As explained in [4], when computing sufficiently smooth solutions using $\mathbf{P}_{\mathbf{k}}^{*}\ P_{\mathbf{k}}$ space configurations based on affine regular meshes, optimal convergence rates of identical approximation orders $k+1$ are obtained for primal and dual variables, as well for $\nabla \cdot \boldsymbol{\sigma}$. For the $\mathbf{P}_{\mathbf{k}}^{**}\ P_{\mathbf{k}+1}$ configuration, higher convergence rate of order $k+2$ is obtained for the primal variable. Furthermore, after static condensation is applied, the condensed systems to be solved only involve the flux edge terms and a constant value for u in each element, and thus they have the same dimension in both configuration cases.

Test Problem The problem is defined over the domain of $\Omega = [0,1] \times [0,1]$, and the load function f is chosen such that the model problem has exact solution given by

$$u(x,y) = \frac{\pi}{2} - \arctan\left[\alpha\left(\sqrt{(x-1.25)^2 + (y+0.25)^2} - \frac{\pi}{3}\right)\right],$$

having strong gradients with magnitude determined by the parameter $\alpha = 200$ in the proximity to the circumference centred at the point $(1.25, -0.25)$, with radius $\pi/3$. Plots of the exact solution $u(x,y)$ and its gradient magnitude are presented in Fig. 1.

Adaptive *hp*-Refinement Process We consider a sequence of *hp*-adaptive meshes with either quadrilateral or triangular geometries, with variable polynomial degree distributions. To construct them, firstly, split the domain into two regions: the region near the singularity and the smooth part, elsewhere. In the region where the solution is smooth, p refinement is adopted in order to produce exponential convergence rates there. In the central region, *hp* refinement is employed in order to generate approximation spaces which better capture the singular behaviour. The initial mesh is composed of uniform elements with mesh size 2^{-3}, and $p = 2$ in the smooth part, and mesh size 2^{-4} and $p = 3$ in the region of the singularity. Then, the refinement process follows a sequence of steps $\ell = 2, 3$, and 4 by first increasing by 1 the

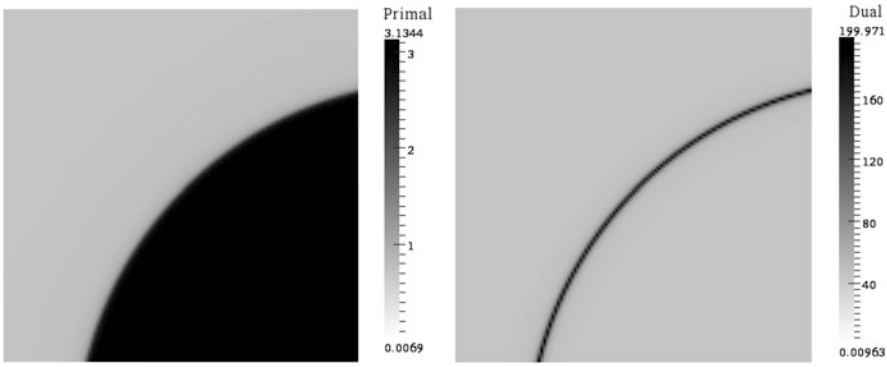

Fig. 1 Exact solution: primal (*left side*) and dual (*right side*) variables

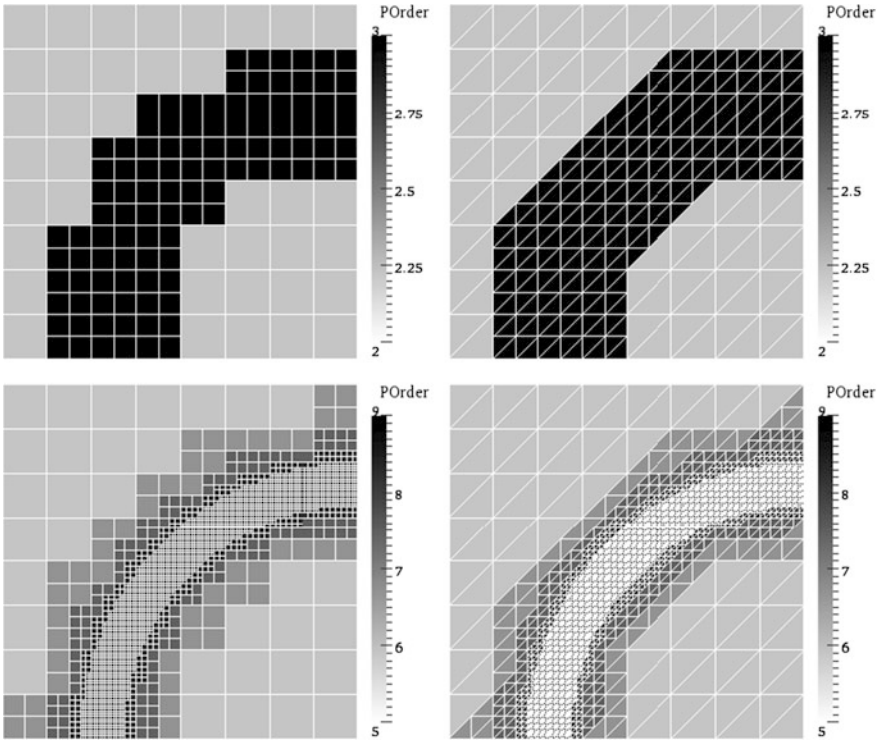

Fig. 2 Illustration of the *hp* refinement process: initial mesh (*top-side*), and mesh at the final refinement step (*bottom-side*) for quadrilateral (*left-side*) and triangular (*right-side*) geometries

approximation order of all elements of the previous step, and then by subdividing the elements intersecting a layer of diameter $2^{-\ell}$ around the singularity curve, and by further increasing their approximation order by 1. Figure 2 illustrates the *hp* refinement process at the initial step, and at the final refinement level.

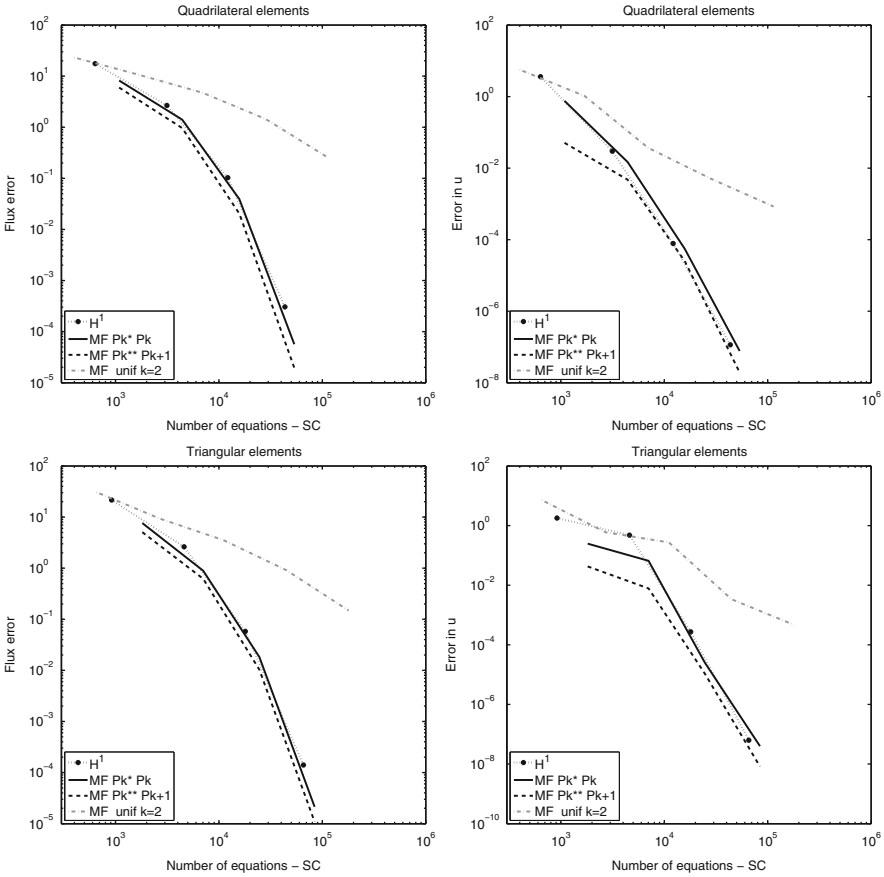

Fig. 3 L^2-error curves in terms of the number of degrees of freedom for the dual (*left side*) and primal (*right side*) variables using mixed formulation and approximation spaces of type $\mathbf{P}_\mathbf{k}^* \; P_\mathbf{k}$ (*continuous curves*), and $\mathbf{P}_\mathbf{k}^{**} \; P_{\mathbf{k}+1}$ (*dashed curves*) based on *hp*-meshes with quadrilateral (*top-side*) and triangular (*bottom-side*) geometries. The *dashed-dotted curves* correspond to simulations for uniform meshes with $\mathbf{P}_\mathbf{2}^* \; P_\mathbf{2}$ configuration. For comparison, results for H^1-conforming formulation based on the same *hp*-meshes are also included (*dotted curves*)

Our purpose is to use these kinds of meshes for the simulation of the test problem by the mixed formulations using the space configurations of $\mathbf{P}_\mathbf{k}^* \; P_\mathbf{k}$ and $\mathbf{P}_\mathbf{k}^{**} \; P_{\mathbf{k}+1}$ types. As expected, the application of *hp* refinement to the singular problem improves considerably the performance of the methods, with exponential rates of convergence. Furthermore, the accuracy in the primal variable improves when $\mathbf{P}_\mathbf{k}^{**} \; P_{\mathbf{k}+1}$ configuration is applied in the mixed formulation. Figure 3 shows the calculated L^2-norms of the dual $\boldsymbol{\sigma}$ and primal u errors using these sequences of *hp*-adaptive meshes versus the number of equations solved after static condensation. For comparison, results for the H^1-conforming formulation based on

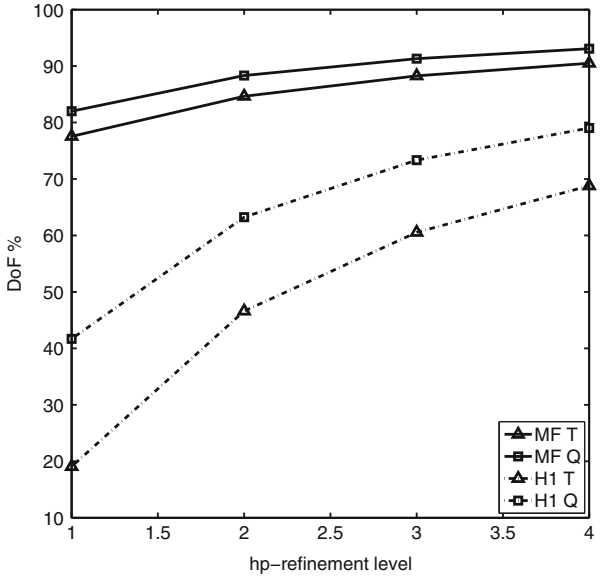

Fig. 4 Percentage of condensed degrees of freedom in the mixed method using the $P_k^* P_k$ space configuration (*continuous lines*) and in the H^1-conforming method (*dashed-dotted lines*), applied to quadrilateral and triangular *hp*-meshes

the same *hp*-meshes, and for the mixed formulation with uniform meshes and $\mathbf{P_2^*}\ P_2$ configuration are plotted. For the experiments with H^1 conforming approximations, the performance in terms of accuracy versus degrees of freedom is similar to the experiments with the mixed formulation.

The effect of static condensation is also verified in terms of the size reduction of the global system to be solved, which is more significant in the mixed formulation, with increasing order of approximation, and with quadrilateral meshes, as compared with triangular ones. At the finest levels of mesh refinement, the number of condensed equations in the mixed formulation amounts to more than 90 %, as shown in Fig. 4, meaning that the size of the condensed system to be solved is less than 10 % of the total number of equations. This fact demonstrates the potential benefit of using **H**(*div*) approximation spaces in parallel computers.

Acknowledgements R. B. Devloo and S. M. Gomes thankfully acknowledge financial support from CNPq – the Brazilian Research Council. The work of A. M. Farias is supported by a pos-doctoral grant by CAPES Foundation, within the Ministry of Education in Brazil. The authors thank T. L. D. Forti for given the adaptive *hp* meshes, and to P. C. A. Lucci for helping with the graphics.

References

1. F. Brezzi, J. Douglas, L.D. Marini, Two families of mixed finite elements for second order elliptic problems. Numer. Math. **47**, 217–235 (1985)
2. F. Brezzi, M. Fortin, *Mixed and Hybrid Finite Element Methods*. Springer Series in Computational Mathematics, vol. 15 (Springer, NewYork, 1991)
3. J.L.D. Calle, P.R.B. Devloo, S.M. Gomes, Implementation of continuous *hp*-adaptive finite element spaces without limitations on hanging sides and distribution of approximation orders. Comput. Math. Appl. **70**(5), 1051–1069 (2015)
4. D.A. Castro, P.R.B. Devloo, A.M. Farias, S.M. Gomes, D. Siqueira, Three dimensional hierarchical mixed finite element approximations with enhanced primal variable accuracy. Comput. Methods Appl. Mech. Eng. **306**, 479–502 (2016)
5. L. Demkowicz, *Polynomial Exact Sequence and Projection-Based Interpolation with Application Maxwell Equations*, ed. by D. Boffi, L. Gastaldi. Mixed Finite Elements, Compatibility Conditions and Applications, Lecture Notes in Mathematics, vol. 1939 (Springer, Heidelberg, 2007), pp. 101–158
6. P.R.B. Devloo, A.M. Farias, S.M. Gomes, D. Siqueira, Two-dimensional *hp*-adaptive finite element spaces for mixed formulations. Math. Comput. Simul. **126**,104–122 (2016)
7. F. Fuentes, B. Keith, L. Demkowicz, S. Nagaraj, Orientation embedded high order shape functions for the exact sequence elements of all shapes. Comput. Math. Appl. **70**(4), 353–458 (2015)
8. J.C. Nedelec, A new family of mixed finite elements in $\mathbb{R}^3$. Numer. Math. **50**, 57–81 (1986)
9. D. Siqueira, P.R.B. Devloo, S.M. Gomes, A new procedure for the construction of hierarchical high order H(div) and H(curl) finite element spaces. J. Comput. Appl. Math. **240**, 204–214 (2013)
10. P. Solin, K. Segeth, I. Dolezel, *Higher-Order Finite Element Methods* (Chapman – Hall/CRC, Boca Raton, 2004)
11. S. Zaglamayr, Hight order finite element methods for electromagnetic field computation. Ph.D. thesis, Johannes Keppler Universität Linz, 2006